

## Towards a quantification of disorder in materials: Distinguishing equilibrium and glassy sphere packings

T. M. Truskett,<sup>1</sup> S. Torquato,<sup>2,\*</sup> and P. G. Debenedetti<sup>1</sup>

<sup>1</sup>*Department of Chemical Engineering, Princeton University, Princeton, New Jersey 08544*

<sup>2</sup>*Department of Chemistry and Princeton Materials Institute, Princeton University, Princeton, New Jersey 08544*

(Received 1 March 2000)

This paper examines the prospects for quantifying disorder in simple molecular or colloidal systems. As a central element in this task, scalar measures for describing both translational and bond-orientational order are introduced. These measures are subsequently used to characterize the structures that result from a series of molecular-dynamics simulations of the hard-sphere system. The simulation results can be illustrated by a two-parameter *ordering phase diagram*, which indicates the relative placement of the equilibrium phases in order-parameter space. Moreover, the diagram serves as a useful tool for understanding the effect of history on disorder in nonequilibrium structures. Our investigation provides fresh insights into the types of ordering that can occur in equilibrium and glassy systems, including quantitative evidence that, at least in the case of hard spheres, contradicts the notion that glasses are simply solids with the “frozen in” structure of an equilibrium liquid. Furthermore, examination of the order exhibited by the glassy structures suggests, to our knowledge, a new perspective on the old problem of random close packing.

PACS number(s): 61.20.Ne, 61.43.-j, 81.05.Kf

### I. INTRODUCTION

A well-developed theoretical and experimental framework is available for studying the structure of regular crystalline solids [1]. In contrast, much less is understood about quantifying the structure of amorphous materials, despite the fact that nature exhibits disorder on a variety of different length scales. Examples range from liquids, gases, and amorphous solids to porous rocks, dispersions, soil, and biological materials such as tissue. In such systems, it is natural to ask the following question: To what extent can we quantify the degree of order (or disorder) present in the sample? In other words, is it possible to develop sensitive numerical measures, so-called *order parameters*, which can detect the presence of order in a system? In addition to their potential viability as scientific tools, methods for quantifying disorder promise to play a role in emerging technological developments. Some of the most important examples can be found in recent medical applications, where it is known that the complex microstructures found in biological materials such as bone, tissue, microblood vessels, and vehicles for drug delivery, are vital for understanding processes ranging from tumor growth [2] to the permeation of drugs into the skin [3].

Central to the idea of describing disorder is understanding the relative placement of different materials in some relevant order-parameter space. It is clear, on the one hand, that a truly random system, by virtue of its definition, exhibits no positional, orientational, or conformational correlations; i.e., its structure is that of an ideal gas. On the other hand, a regular crystalline array is a manifestation of perfect order. Our experience with real world materials, which are subject to thermal agitation and structural defects, indicates that these two extremes are only abstract limiting concepts. Be-

tween the ideal gas and the perfect crystal, lie imperfect gases, liquids (both stable and metastable), glasses, defective crystals, and structures that evolve from nonequilibrium processes, such as irreversible adsorption onto a surface. Depending on the point of view, all such systems exhibit a certain degree of order (or disorder), and the differences between them can be quite subtle. For instance, the classic problem of distinguishing between the structures of dense glasses and polycrystalline materials remains a significant challenge to materials scientists and engineers [4,5].

The characterization of disordered materials is a particularly difficult task because any reasonably compact description of their structure is necessarily statistical in nature. Such detailed statistical information can be written down exactly for completely random or uncorrelated systems (ideal gases) [6] in any spatial dimension  $D$ . However in real materials, interactions with other particles, container boundaries, or external fields such as gravity can cause significant deviations from randomness, which ultimately manifest themselves in the form of spatial correlations.

The simplest nontrivial model that exhibits strong correlations is the one-dimensional ( $D=1$ ) hard-rod fluid, also known as the Tonks gas [7,8]. The rudimentary form of its interatomic potential (pure hard-core repulsion) and its topological simplicity relative to models in two and three spatial dimensions ( $D=2,3$ ) have allowed for a very complete description of its structure. For instance, pair and higher-order correlation functions [9,10], neighbor distributions [11–15], density fluctuations [15], void statistics [16,17], and various aspects of its normal-mode coordinates [18] can be expressed analytically for the equilibrium (and in some cases for nonequilibrium) ensembles. Unfortunately, a comparable wealth of statistical information about the structure of most real and model materials is not available *a priori*. Rather, order parameters must be determined based on structural statistics either measured in an experiment (for instance, via scatter-

\*Electronic address: torquato@matter.princeton.edu

ing, tomography, or microscopy) or calculated directly from a molecular simulation.

For pragmatic purposes, it is desirable if the order parameters to be calculated reduce the available statistical information to scalar measures of order in the material. Simple indices of this sort (e.g., the Rockwell hardness scale [19]) have a long history of providing very practical means for comparing material properties. Recently, we introduced a set of scalar order parameters to quantify disorder in random packings of spheres and discussed the utility of these measures for general many-body systems, including liquids and solids [20]. In the present paper, we explore the behavior of such measures to quantify different aspects of ordering in simple molecular or colloidal systems. These ordering metrics facilitate the introduction of a new concept, the two-parameter *ordering phase diagram*, which illustrates the relative placement of a material's equilibrium phases in order-parameter space. Perhaps more importantly, we notice that the ordering-phase diagram can also serve as a means for mapping the degree of order in nonequilibrium (or history-dependent) structures as a function of their processing conditions.

We demonstrate the utility of these new concepts by studying in detail the structure of the three-dimensional hard-sphere system via a series of molecular-dynamics simulations. The hard-sphere system is an ideal starting point for quantifying disorder in materials because it represents the simplest model material that exhibits both a first-order freezing transition and a glass transition. Moreover, it is known (see, e.g., Ref. [21]) that the structures exhibited by many ‘‘real’’ metallic glasses (such as  $\text{Ni}_{65}\text{B}_{35}$ ,  $\text{Ni}_{62}\text{Nb}_{38}$ , and  $\text{Pd}_{52}\text{Ni}_{32}\text{P}_{16}$ ) can be adequately represented by dense random packings of hard spheres.

In order to quantify the degree of ordering that is exhibited by the hard-sphere system, we analyze structures from the equilibrium fluid, the equilibrium crystal, and a series of glasses produced by varying compression schedules. We find that the results of these calculations provide us with a reference ordering-phase diagram, and herein we discuss the possibility of extending these calculations to investigate further the connection between intermolecular interactions and ordering. Finally, we note that our detailed investigation of glassy packings supports a reassessment of the traditional notion of the random close-packed state.

This paper is organized as follows. In Sec. II we introduce two simple order parameters for substances that are known to freeze into a face-centered-cubic crystal. In Sec. III we use these order parameters to analyze ensembles of equilibrium and nonequilibrium structures in the hard-sphere system, and we illustrate these results via a set of ordering phase diagrams. Furthermore, we demonstrate how the ordering phase diagram can be used as a tool for understanding the effect of history on disorder in nonequilibrium structures. In Sec. IV we introduce two ‘‘general’’ order parameters that do not require a specific crystalline structure as an input. These measures reproduce qualitatively the features of the original ordering phase diagram and suggest the possibility of a universal description for simple systems. Finally, in Sec. V we present some concluding remarks.

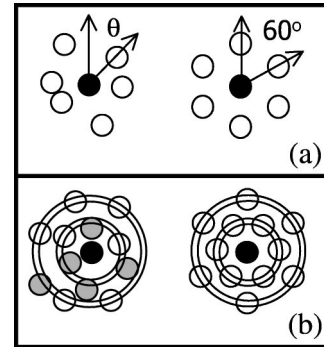


FIG. 1. Two types of ordering that occur in simple systems. (a) Bond-orientational order. This measure contains information about the orientation of the vectors connecting neighboring particles in the sample (left). If these orientations persist throughout the structure, as they do in a perfect crystal (right), then the system is considered to be bond orientationally ordered. (b) Translational order. This measure contains information about the relative spacing of particles in the system of interest (left) relative to some relevant crystalline lattice at the same density (right).

## II. ORDER PARAMETERS

Perhaps one of the most intuitive means for describing order in a material is to compare the structure of that material to some relevant crystalline lattice at the same density. For the order parameters considered in Sec. II, we focus on systems that are known to freeze into the face-centered-cubic (fcc) crystal. As is well-known, the fcc structure is the stable crystalline phase for a number of metals, rare gases, and model systems comprising particles that exhibit steep repulsive forces (e.g., the Lennard-Jones and hard-sphere fluids). The ideas presented in this section are generalized in Sec. IV, where two new measures are introduced that do not require a specific reference crystal structure as an input.

For a collection of spherically symmetric particles, there are two relatively basic scalar measures of order: *translational order* and *bond-orientational order* (Fig. 1). The former measure contains information about the average relative spacing of the particles; i.e., it detects the extent to which certain positions in space are preferentially occupied. The latter measure, bond-orientational order [22], contains information about the spatial orientation of vectors connecting the centers of neighboring particles. When the orientations of these imaginary bonds persist over macroscopic distances in the sample (as they do in a perfect crystal), then the material is said to be bond-orientationally ordered. This should not be confused with *molecular orientational order*, which describes the persistence of preferential orientations of *anisotropic* particles in a material.

Steinhardt *et al.* [23] have introduced a set of bond-orientational order parameters that are particularly sensitive to the overall degree of crystallinity in the system. For these measures, one is obliged to ascribe to each particle  $i$  a set of nearest neighbors. Here, we have defined the set of neighbors to particle  $i$  to be all particles  $j$  that lie within a radial distance  $r_{ij}$  of the central particle such that  $0 \leq r_{ij} \leq r_{\min}$ , where  $r_{\min}$  is the first minimum in the radial distribution function  $g(r)$  [24]. Historically, the vectors  $\mathbf{r}_{ij}$  connecting nearest neighbors, oriented along unit vectors  $\hat{\mathbf{r}}_{ij}$ , are called ‘‘bonds.’’ The spatial orientations of these bonds with re-

spect to an arbitrary reference axis are uniquely determined by the polar and azimuthal angles  $\theta_{ij}$  and  $\phi_{ij}$ . To construct invariants, one begins by assigning the spherical harmonics  $Y_{lm}$ :

$$Q_{lm}(\hat{\mathbf{r}}_{ij}) = Y_{lm}(\theta_{ij}, \phi_{ij}) \quad (2.1)$$

to each bond oriented in a direction  $\hat{\mathbf{r}}_{ij}$ . These values are subsequently averaged over all bonds in the sample to obtain the *global* orientational order parameters  $\overline{Q_{lm}}$ :

$$\overline{Q_{lm}} = \langle Q_{lm}(\hat{\mathbf{r}}_{ij}) \rangle. \quad (2.2)$$

The quantity  $\overline{Q_{lm}}$  still depends on the choice of the reference frame. However, one can form the combination  $Q_l$ :

$$Q_l = \left( \frac{4\pi}{2l+1} \sum_{m=-l}^{m=l} |\overline{Q_{lm}}|^2 \right)^{1/2}, \quad (2.3)$$

which is a rotationally invariant measure. In our studies, we will be interested in  $Q_6$ , which has the ideal property that it should be  $1/\sqrt{N_b}$  for a completely uncorrelated sample (ideal gas), where  $N_b$  is the total number of bonds in the system. Moreover,  $Q_6$  is significantly larger when crystallites are present in the system, and it attains its maximum value for space-filling structures in the perfect fcc crystal. For the purposes of this paper, we normalize  $Q_6$  by its value in the perfect fcc crystal  $Q_6^{\text{fcc}} = 0.57452$  to obtain

$$Q = \frac{Q_6}{Q_6^{\text{fcc}}}. \quad (2.4)$$

Note that our normalized bond-orientational order parameter  $Q$ , in the infinite volume limit, scales between 0 (complete disorder) and 1 (perfect fcc ordering); thus, it effectively serves as a ‘‘meter’’ for crystallization in the sample. Moreover,  $Q$  is quite large for other common space-filling structures ( $Q = 0.6154$ ,  $0.8438$ , and  $0.8887$  for simple cubic, hexagonally-close-packed, and body-centered-cubic structures, respectively).

In contrast to the bond-orientational order parameters mentioned above, scalar measures of translational order have not been well studied. We have recently introduced a translational order parameter  $T$  that measures the degree of spatial ordering in the system of interest, relative to the perfect fcc lattice at the same density [20]. Specifically,

$$T = \frac{\left| \sum_{i=1}^{N_C} (n_i - n_i^{\text{ideal}}) \right|}{\left| \sum_{i=1}^{N_C} (n_i^{\text{fcc}} - n_i^{\text{ideal}}) \right|}, \quad (2.5)$$

where  $n_i$  (for the system of interest) indicates the average occupation number for the spherical shell of width  $a\delta$  located at a distance from a reference sphere that equals the  $i$ th nearest-neighbor separation for the open fcc lattice at that density,  $a$  is the first nearest-neighbor distance for that fcc lattice, and  $N_C$  is the total number of neighbor shells considered (see Fig. 1). Similarly,  $n_i^{\text{ideal}}$  and  $n_i^{\text{fcc}}$  are the corresponding neighbor shell occupation numbers for an ideal gas

(spatially uncorrelated spheres) and the open fcc crystal lattice, respectively. In our study, we chose to consider the first seven neighbor shells ( $N_C = 7$ ), utilizing a shell-width parameter of  $\delta = 0.196$ . Our tests indicate that the consideration of more neighbor shells does not result in qualitatively different behavior for  $T$ . It is worth noting that, like the bond-orientational order parameter  $Q$ , the translational order parameter  $T$  scales between 0 (complete disorder) and 1 (perfect fcc spatial ordering).

Both order parameters, i.e.,  $T$  and  $Q$ , should be generally applicable to simple atomic or colloidal fluids [25] that are known to freeze into the fcc crystal. In Sec. III, we utilize these measures to investigate ordering in the hard-sphere system.

### III. ORDERING IN THE HARD-SPHERE SYSTEM

#### A. Simulation details

In order to generate a representative set of structures in the hard-sphere system, we have carried out a series of molecular-dynamics simulations of 500 identical hard spheres in the canonical ensemble, using a cubic box with periodic boundary conditions. In these simulations, we have analyzed configurations from the equilibrium fluid, the equilibrium fcc crystal, and a set of history-dependent glassy structures produced by the well-known method of Lubachevsky and Stillinger [26–28].

Glassy structures created from the Lubachevsky-Stillinger protocol are termed history dependent because their properties depend explicitly on the initial conditions of the fluid and the rate of densification. Specifically, the procedure is initialized with a set of sphere positions and velocities that are extracted from a ‘‘snapshot’’ of the equilibrium fluid at low density. Then, during the course of an otherwise standard constant-volume molecular-dynamics simulation, the sphere diameter  $\sigma(t)$  is increased linearly in time  $t$ . The process terminates in a *jammed state* in which  $\sigma(t)$  can no longer increase in time without sphere overlap, the collision rate diverges, and no further densification can be achieved without first decompressing and relaxing the system. We identified the jammed state as having occurred when the sphere diameters stabilized despite continuing collisions [26]. We note in passing that the collision dynamics of this compression protocol differ from conventional elastic sphere dynamics because the colliding spheres must be given an extra impetus, along the line connecting their centers, to ensure that their surfaces are moving apart after the collision. The details of the alternative dynamics are relatively easy to implement and are outlined in the original reference [26].

The dimensionless compression rate  $\Gamma$  is given by

$$\Gamma = \left( \frac{d\sigma(t)}{dt} \right) \sqrt{\frac{m}{k\theta}}, \quad (3.1)$$

where  $m$  is the mass of a sphere,  $k$  is Boltzmann’s constant, and  $\theta$  is the temperature. Note that the compression rate  $\Gamma$  controls the processing history for the hard-sphere glasses formed by this protocol, and its role is analogous to that of the cooling schedule in experimental glasses. In fact, Speedy [29] has recognized that the dimensionless compression rate  $\Gamma$  is related to a laboratory (isobaric) cooling rate  $(\partial\theta/\partial t)_p$ :

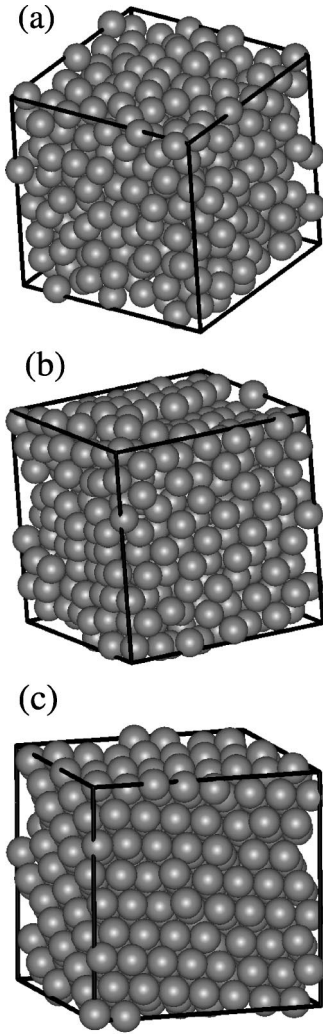


FIG. 2. Glassy structures generated using the Lubachevsky-Stillinginger protocol. Structures are shown with packing fractions (a)  $\phi=0.646$ , (b)  $\phi=0.667$ , and (c)  $\phi=0.692$  generated from dimensionless compression rates  $\Gamma=0.01$ , 0.001, and 0.0005, respectively.

$$\left(\frac{\partial\theta}{\partial t}\right)_P = -3\Gamma\theta\left(\frac{d\ln[P/\rho_{cp}k\theta]}{d\ln\rho}\right)\sqrt{\frac{k\theta}{m\sigma^2}}, \quad (3.2)$$

where  $P$  is the pressure,  $\rho=N/V$  is the number density,  $\rho_{cp}=\sqrt{2}/\sigma^3$  is the number density for the close-packed fcc crystal,  $N$  is the number of spheres, and  $V$  is the system volume. Using Speedy's estimate [29] from molecular simulations  $d\ln[P/\rho_{cp}k\theta]/d\ln\rho\approx 4.7$  at  $\rho=1.1\sigma^{-3}$ , a temperature of  $\theta=273$  K, and both the stoichiometrically averaged mass  $m=19.95$  g/mole and the effective hard-sphere radius  $\sigma=2.025$  Å [21] for  $\text{Ni}_{65}\text{B}_{35}$  yields an estimated quench rate of  $(\partial\theta/\partial t)_P\approx -6\Gamma\times 10^{15}$  K/s. In this paper, we focus on dimensionless compression rates that span the range  $10^{-4}<\Gamma<10^{-2}$ , corresponding roughly to cooling rates in a range  $(10^{12}\text{ K/s}<(\partial\theta/\partial t)_P<10^{14}\text{ K/s})$ , values which are typical for molecular simulations [30]. We note that while many standard techniques for metallic glass production (e.g., melt spinning) generate more modest cooling rates (of the

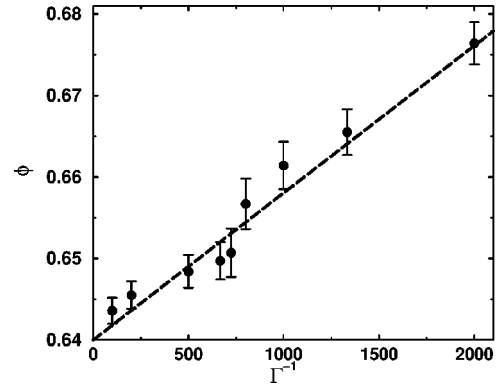


FIG. 3. Final packing fraction  $\phi$  in the glassy structures as a function of reciprocal compression rate  $\Gamma^{-1}$ . The black circles represent an average of 27 glasses produced at each rate. The dashed line is a linear fit to the data.

order  $10^5$ – $10^6$  K/s [31]), very thin surface layers can be quenched at ultrarapid rates ( $10^{14}$  K/s) by pulsed laser quenching [32].

The amount of computation time required for executing the Lubachevsky-Stillinginger compressions can be significantly reduced if the runs are initiated from equilibrium fluid configurations at a finite packing fraction  $\phi$  (in this case we chose  $\phi=0.30$ ). Here,  $\phi$  is defined as the fraction of the total volume  $V$  occupied by the  $N$  spheres, i.e.,  $\phi=\pi\sigma^3N/6V$ . We have found that the glassy structures formed from this initial condition are virtually indistinguishable from glasses compressed at the same rate  $\Gamma$  from the ideal gas, i.e.,  $\sigma(t=0)=0$ .

### B. Hard-sphere glasses

Three-dimensional representations of typical glassy structures generated by a variety of compression rates are shown in Fig. 2. The first structure [Fig. 2(a)] is a glassy packing that was generated using a dimensionless compression rate of  $\Gamma=0.01$ . It has a packing fraction of  $\phi=0.646$ , which roughly corresponds to what has been traditionally termed the *random close-packed state* (see, e.g., [33]), and appears to be quite amorphous. Denser jammed structures can be formed in the hard-sphere system [see Figs. 2(b) and 2(c)] by reducing the compression rate and thereby allowing the spheres to find more compact configurations. This increase in density, however, is achieved at the expense of increased order in the sample.

The dependence of the limiting packing fraction  $\phi$  on the reciprocal compression rate  $\Gamma^{-1}$  is illustrated in Fig. 3. Shown are the average packing fractions obtained from 27 compressions at each of 9 different compression rates. It is clear that slow compressions result in packings that are both very dense and [as can be deduced from Fig. 2(c)] conspicuously ordered. In fact using extremely slow rates ( $\Gamma<10^{-4}$ ), we have produced fcc crystals by the Lubachevsky-Stillinginger protocol that were within 1% of the close-packed limit of  $\phi_{CP}=\pi/(3\sqrt{2})\approx 0.74$  (not shown in Fig. 3). In contrast, rapid compressions create lower density, more disordered packings. A linear fit to the data in Fig. 3 extrapolates to a packing fraction of  $\phi\approx 0.64$  in the limit of infinite compression rate.

In the context of equilibrium (or metastable) hard-sphere systems, one generally considers two natural limiting high-density states: the fcc close-packed structure ( $\phi = \sqrt{2}\pi/6 \approx 0.74$ ) and the random close-packed state ( $\phi \approx 0.64$ ). However, Fig. 3 clearly demonstrates that these limiting states for the hard-sphere system represent a very small subset in a virtual *continuum* of jammed structures that span the high-density range  $0.64 < \phi < 0.74$ . Moreover, we see that the final packing fraction and, subsequently, the degree of ordering in the sphere packings created by the Lubachevsky-Stillinger protocol can be statistically controlled by the compression rate  $\Gamma$ .

It should be noted that the jammed hard-sphere structures with the lowest density for spatial dimensions  $D > 1$  have yet to be identified. A number of interesting examples of low-density jammed structures for  $D=2$  (hard disks) have been noted by Lubachevsky *et al.* [27]. For  $D=3$  (hard spheres), the close-packed cubic lattice (contained by rigid boundaries) with a packing fraction of  $\phi = \pi/6 \approx 0.52$ , is an obvious example, but it is most likely not the lowest-density jammed structure. To investigate this interesting open issue, we are currently developing simulation techniques for generating jammed hard-sphere packings in the low-density range ( $\phi < 0.64$ ).

### C. Ordering phase diagrams

An interesting question to pose about a given material is the following: How do its various equilibrium and glassy structures rank in terms of the degree of order they exhibit? In other words, for a system with a given intermolecular potential, our goal is to construct a diagram that illustrates the relative placement in order parameter space of the equilibrium and nonequilibrium structures. Figure 4 illustrates two such ordering phase diagrams for the hard-sphere system. In particular, the dependence of the translational and bond-orientational order parameters,  $T$  and  $Q$ , on packing fraction  $\phi$  (as measured in our molecular dynamics simulations) is plotted for the equilibrium liquid, the equilibrium fcc crystal, and the series of history-dependent glasses from Fig. 3.

As should be expected, the translational order parameter  $T$  in the equilibrium fluid vanishes at low density. However,  $T$  increases monotonically as the system is compressed toward the freezing transition ( $\phi_f \approx 0.494$ ), indicating that the increase in density imparts a significant amount of short-range order to the fluid. A discontinuous jump in the order parameter is observed upon freezing to the equilibrium crystal, as is consistent with a first-order phase transition. In the crystal,  $T$  is less than unity at the melting point ( $\phi_m \approx 0.545$ ) because of thermal motion, but the crystal becomes increasingly ordered as it is compressed, approaching  $T=1$  for the close-packed fcc structure at  $\phi_{CP} \approx 0.74$ .

Having established the relative placement of the equilibrium phases on the ordering phase diagram, one can begin to consider plotting the positions of the nonequilibrium structures on the diagram *as a function of their processing conditions*. Figure 4(a) illustrates the effect of compression rate  $\Gamma$  on both the translational ordering  $T$  and the packing fraction  $\phi$  of the glassy structures generated from the Lubachevsky-Stillinger protocol. There are two salient fea-

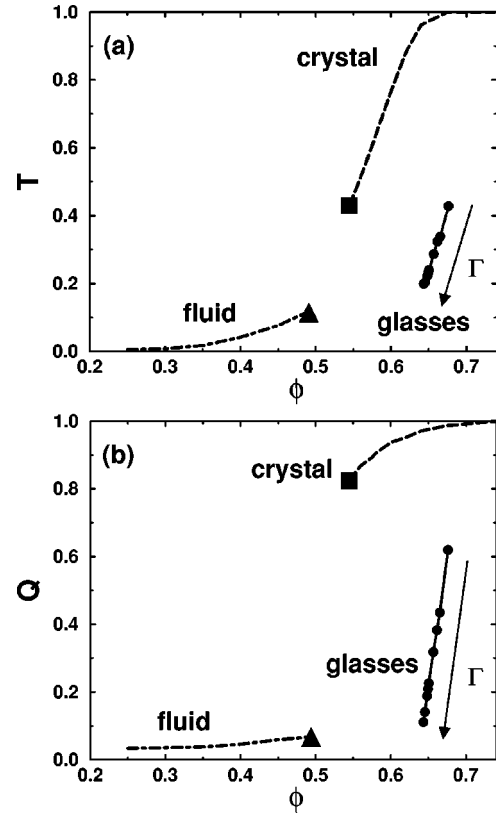


FIG. 4. Ordering phase diagrams for the hard-sphere system. (a) Translational order parameter  $T$  vs packing fraction  $\phi$ . Shown are the equilibrium fluid (dot dashed), the equilibrium fcc crystal (dashed), and the set of history-dependent glasses (circles) from Fig. 3. The degree of ordering in the coexistence region can be determined by a simple lever rule (not shown). Note that both the degree of order and the final packing fraction of the glassy structures can be statistically controlled by the compression rate  $\Gamma$ . The freezing and melting transitions are indicated by the black triangle and black square, respectively. (b) Bond-orientational order parameter  $Q$  vs packing fraction  $\phi$ . Symbols are identical to those presented in (a).

tures of the glassy structures in this plot. First, the amount of translational order in the glasses can be statistically controlled by the compression rate. Second, there is no unambiguous division between amorphous and polycrystalline packings; i.e., ordering in jammed structures is a matter of degree.

It is interesting to note that the random close-packed state has historically been considered to be the *densest amorphous packing* that a collection of spheres can attain. However, our simulation results indicate that this definition cannot be made mathematically precise in light of the fact that one can always create slightly denser packings at the expense of small increases in order. In another paper [20], we demonstrated how the ordering phase diagram suggests replacing the well-accepted notion of random close-packing with a new concept, termed the *maximally random jammed state*, which can be made precise and provides fresh insights into the nature of disorder in glassy systems.

Figure 4(b) is the ordering phase diagram for the bond-orientational order parameter  $Q$  in the hard-sphere system [34]. Notice that the density dependence of  $Q$  is qualitatively similar to that of the translational order parameter  $T$ .

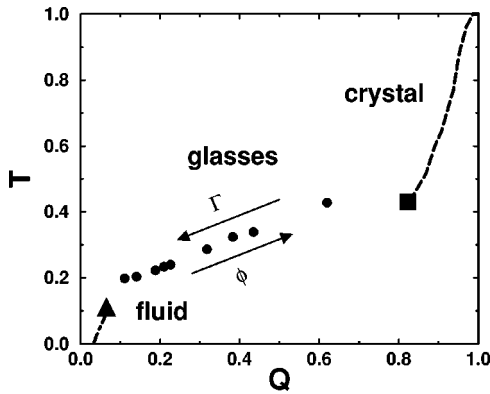


FIG. 5. Two-parameter ordering map for the hard-sphere system. Shown are the coordinates in order parameter space ( $T, Q$ ) for the equilibrium fluid (dot dashed), the equilibrium fcc crystal (dashed), and the set of history-dependent glasses (circles) from Fig. 3. Along each of these sets, packing fraction  $\phi$  increases from left to right. Unlike the equilibrium state points, the positions of the glassy structures in order parameter space are determined by the processing conditions (in this case, the compression rate  $\Gamma$ ). As in Fig. 4, the freezing and melting transitions are indicated by the black triangle and black square, respectively.

Namely, we see minimal ordering in the equilibrium fluid, a discontinuous jump in the order parameter upon freezing, and a crystal whose degree of order systematically increases with packing fraction  $\phi$ . Moreover, the behavior of  $Q$  affirms the conclusion that glassy packings can span from “liquid-like” to “crystal-like” configurations, with the precise degree of order in the jammed structures being statistically controlled by the compression rate  $\Gamma$ .

We can gain some further insight into the nature of ordering in the hard-sphere system by studying the correlation between translational and bond-orientational order in various structures. Practically speaking, this can be accomplished by constructing a *two-parameter order map* ( $T$  vs  $Q$ ) which illustrates the relative placement in order parameter space of the equilibrium phases and the nonequilibrium glassy structures (see Fig. 5). One striking feature of the order map shown in Fig. 5 is the strong positive correlation that exists between  $T$  and  $Q$  for the equilibrium fluid and crystalline phases. In addition, we see that the fluid and the fcc crystal are separated by a large gap in order parameter space that serves as a “no man’s land” for the pure equilibrium phases. Interestingly, packings that exhibit coordinate pairs  $(T, Q)$  in the no man’s land can be generated if we resort to nonequilibrium methods of preparation such as the Lubachevsky-Stillinger compression protocol.

The notion that there is a large region of order parameter space ( $0.15 < T < 0.40$  and  $0.1 < Q < 0.8$ ) populated by the glassy structures but not visited with any statistical significance by the pure equilibrium phases, is very intriguing. In other words, the degree of order exhibited by the sphere centers in the glassy packings is noticeably greater than that of the equilibrium fluid at the freezing transition and, simultaneously, less than that exhibited by the equilibrium fcc crystal at the same packing fraction  $\phi$ . This indicates that certain nonequilibrium packings can be distinguished from the equilibrium system based on *structural information alone*, e.g.,  $T$  and  $Q$ . Moreover, the results seems to contra-

dict (at least for the hard-sphere system) the commonly held notion that glasses are simply solids with the “frozen in” structure of an equilibrium liquid [35]. It is important to realize that, since temperature plays a trivial role in hard-body systems, hard-sphere glasses must be formed by compression and *necessarily have a higher packing fraction  $\phi$  than the corresponding equilibrium fluid*. Nevertheless, it is reasonable to expect that a similar degree of ordering would arise in glasses formed by the rapid cooling of a dense simple liquid (e.g., the Lennard-Jones fluid), where the structure is dominated by repulsive forces. Of course, the extent to which these results can be extended to systems with attractive interactions is an interesting open question which merits further investigation.

In this paper, we note that the nonequilibrium glassy structures are *more ordered* than those found in the equilibrium fluid. In fact this result was anticipated in an earlier paper [36], where it was shown that the familiar split-second peak seen in hard-sphere glasses develops from a weaker shoulder in the equilibrium fluid and is associated with a substantial increase in orientational ordering. We note in passing that by biasing the system, one can construct an ensemble of nonequilibrium hard disk packings ( $D=2$ ) that are significantly *more disordered* than the corresponding equilibrium fluid structures at the same packing fraction [37].

Although we have concentrated on a highly idealized model system in this paper, the two-parameter order map suggests some challenging scientific questions about real materials and indicates several specific areas that deserve further investigation. First of all, it is clear that there exist large sets of coordinate pairs  $(T, Q)$  in order parameter space, i.e., certain types of ordering, which for some systems are completely (or at least statistically) inaccessible. Can we understand the relationship between these inaccessible regions and the relevant interactions in the system? Moreover, can we use the order map as a general guide for classifying the relationship between the morphology of more complicated glassy systems and their processing history? What if a material’s crystal structure is unknown? We are currently investigating the first two questions in our research, while the third question is the subject of Sec. IV in this paper.

#### IV. CRYSTAL-INDEPENDENT MEASURES

Up to this point, we have relied on the notion that ordering in a system should be measured relative to some specific crystal structure. This approach, while useful for the simple systems we have considered, is less than satisfactory for materials with either multiple crystalline phases or for which the crystal structure is unknown. In these more complicated systems, one must generally find measures that have the ability to detect the presence of growing spatial correlations in the system without *a priori* knowledge about the structure of the crystalline phase. In this section, we present two very simple examples of prospective crystal-independent measures and compare them to the translational and orientational metrics introduced in Sec. II.

The first quantity that we consider is a translational order parameter  $T^*$ , which provides a measure of the local-density modulations in the system

$$T^* = \frac{\int_{\rho^{1/3}\sigma}^{\xi_C} |h(\xi)| d\xi}{\xi_C - \rho^{1/3}\sigma}. \quad (4.1)$$

Density-density correlations are detected with this measure by integrating over the absolute value of the total correlation function  $h(\xi) = g(\xi) - 1$ , where  $g(\xi)$  is the radial distribution function,  $\xi = r\rho^{1/3}$  is the radial coordinate  $r$  scaled by the cube root of the number density  $\rho = N/V$ , and  $\xi_C$  is a numerical cutoff which is limited by the size of the simulation box (for our simulations, we chose  $\xi_C = 3.5$ ). Here, we have taken the liberty of using the rescaled radial coordinate  $\xi$  so that the integral appearing in Eq. (4.1) sums over an equivalent number of coordination shells at each density.

Note that for systems comprising molecules with attractive interactions, the total correlation function  $h(r)$  becomes long-ranged in the vicinity of the liquid-vapor critical point. This may result in an increase in  $T^*$ , defined by Eq. (4.1), when in fact no significant molecular ordering will have occurred. Of course, since we are concerned with the hard-sphere system in this paper, the behavior of  $T^*$  in the vicinity of a critical point is of no immediate concern. Nevertheless, understanding the behavior of  $T^*$  near both the freezing transition and the critical point is a crucial step towards determining its general viability as an order parameter, and it is an issue we are currently investigating.

Another interesting statistical quantity that one can measure in a simulation is the two-body excess entropy  $s^{(2)}$  given by (see Refs. [38–40])

$$s^{(2)} = -\frac{k\rho}{2} \int d\mathbf{r} \{g(r) \ln g(r) - [g(r) - 1]\}. \quad (4.2)$$

This measure is essentially the multiparticle correlation function expansion of the excess entropy (relative to an ideal gas at the same density) truncated at the two-body terms. This expression was first derived by Nettleton and Green [38] in the grand-canonical ensemble, and Baranyai and Evans [40] later demonstrated that the quantity is indeed “ensemble-invariant.” When truncated at the two-body terms, the series has been shown to be a reasonable approximation for the full excess entropy in several model liquids [40,41]. It has also been directly measured in simulations of nonequilibrium steady shear flows [42].

Since  $s^{(2)} = 0$  for completely disordered systems (i.e., the ideal gas) and becomes large and negative for ordered structures ( $s^{(2)} \rightarrow -\infty$  for perfect crystalline arrangements), it may seem to provide a practical measure of disorder in the system. In the context of the present paper, we are interested in order parameters, and thus we focus on the dimensionless, positive-definite [43] quantity  $-s^{(2)}/k$ . It should be noted that although the integral appearing in Eq. (4.2) must be truncated when measured in a simulation box of finite size, it is known that the quantity measured will be a lower bound [40] on  $-s^{(2)}$  that is indeed very tight in the liquid phase.

Figure 6 illustrates the ordering phase diagrams for the hard-sphere system prepared using the two order parameters introduced in this section,  $T^*$  and  $-s^{(2)}/k$ . Notice that these measures provide a description of the system that is qualitatively similar to that seen in Fig. 4. Specifically, we see that

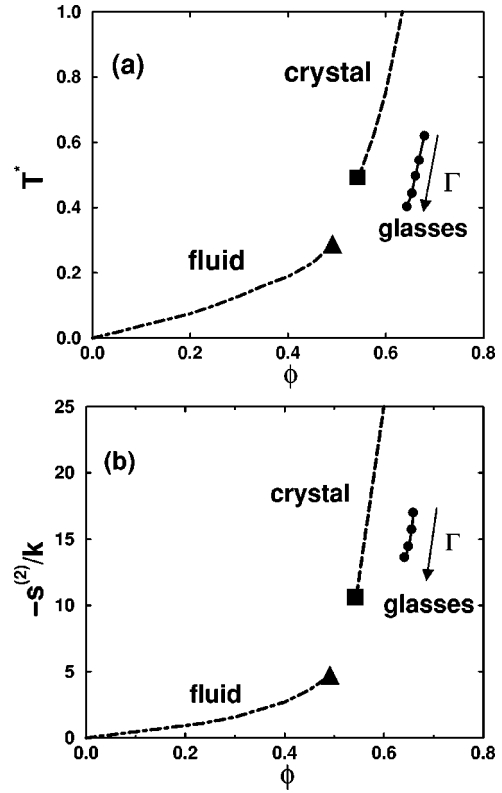


FIG. 6. Ordering phase diagrams for the hard-sphere system using the crystal-independent measures introduced in the text. (a) Alternative translational order parameter  $T^*$  versus packing fraction  $\phi$ . Shown are the equilibrium fluid (dot dashed), the equilibrium fcc crystal (dashed), and a set of glasses (circles) whose structure depends on the compression rate  $\Gamma$ . The freezing and melting transitions are indicated by the black triangle and black square, respectively. (b) The magnitude of the excess (two body) statistical entropy  $-s^{(2)}/k$  versus packing fraction  $\phi$ . Symbols are identical to those presented in (a).

both measures indicate a low degree of ordering in the equilibrium fluid, a discontinuous jump in the order parameter upon freezing into the crystal, and an equilibrium crystal whose degree of order systematically increases with packing fraction  $\phi$ . Once again, the order parameter plots indicate that the degree of order and the packing fraction  $\phi$  in the glassy structures can be statistically controlled by the compression rate  $\Gamma$ .

One important caveat concerning  $s^{(2)}$  is its inability to distinguish between certain basic varieties of sphere packings. As can be seen in Eq. (4.2), the presence of delta functions in the radial distribution function  $g(r)$ , will result in a divergence in the two-body entropy ( $s^{(2)} \rightarrow -\infty$ ). This divergence, which is a well-known feature of the entropy in highly compressed, classical rigid particle systems [44], limits the utility of  $s^{(2)}$  as an order parameter in many cases. For instance, the two-body entropy will not be able to distinguish between alternative perfect crystal structures and a number of hard-sphere packings in the ideal “jamming” limit [20].

As a final remark, we note that the order parameters, introduced in this paper, by no means exhaust the possibilities even for simple systems. For instance, we have focused only on the “global” versions of the translational and bond-orientational order parameters  $T$  and  $Q$ . Clearly one can ex-

amine “local” versions of these quantities  $t$  and  $q$  and their associated spatial correlations. For instance, we can define a local version  $t$  of the global translational order parameter  $T$  given by Eq. (2.5) for each atom in the system

$$T_L = \left| \frac{\sum_{i=1}^{N_C} (n_i - n_i^{ideal})}{\sum_{i=1}^{N_C} (n_i^{fcc} - n_i^{ideal})} \right|. \quad (4.3)$$

Using this local definition, a correlation function  $G_t(r)$  can be constructed

$$G_t(r) = \frac{\langle [T_L(0) - \bar{T}_L][T_L(r) - \bar{T}_L] \rangle}{\langle [T_L(0) - \bar{T}_L][T_L(0) - \bar{T}_L] \rangle}, \quad (4.4)$$

where the angular brackets indicate an average over all particles separated by a scalar distance  $r$  and  $\bar{T}_L$  signifies an average over all atoms in the system. By tracking the spatial decay of the correlation between local translational ordering [as is done for  $g(r)$  in Eq. (4.1)], a new measure of translational ordering is obtained. Of course, a similar correlation function can be defined for the local bond-orientational order parameter  $q$  [23]:

$$G_q(r) = \frac{1}{13} \sum_{m=-6}^6 \langle q_{6m}^*(r) q_{6m}(0) \rangle \langle q_{00}^*(r) q_{00}(0) \rangle^{-1}, \quad (4.5)$$

where  $*$  denotes complex conjugation, and the angular brackets indicate an average over all bonds separated by a scalar distance  $r$ . Here, the  $q_{lm}$  are the spherical harmonics computed according to the orientation of each individual bond with respect to an arbitrary reference axis. Once again, the spatial decay of  $G_q(r)$  will provide a measure of the persistence of bond-orientational order in the system.

In either case, since there is no single and complete scalar measure of order in a material, the order parameters one chooses are unavoidably subjective. Nevertheless, it is striking to see that the set of measures presented here give a seemingly unified picture for ordering in the purely repulsive hard-sphere system. Understanding the sensitivity of this picture to changes in intermolecular interactions, therefore, represents the next major challenge for quantifying disorder in condensed-phase systems.

## V. CONCLUDING REMARKS

In this paper, we have explored a set of simple order parameters that allow one to quantify the degree of order (or disorder) in simple molecular or colloidal systems. These

sensitive measures have facilitated the introduction of a new concept, the two-parameter ordering map, which illustrates the relative placement in order parameter space of a material’s equilibrium phases. In addition, the ordering phase diagram allows one to map out the degree of order in history-dependent structures, e.g., glasses, as a function of their processing conditions.

We have demonstrated that there is a large region of the two-parameter ( $T-Q$ ) order parameter space that serves as a no man’s land for the pure equilibrium phases. In other words, there are certain degrees of ordering that are not realized by the hard-sphere system under equilibrium conditions. However, we demonstrate that glassy structures that exhibit this “intermediate” type of order can be produced by nonequilibrium methods such as the compression protocol of Lubachevsky and Stillinger. This contradicts the common notion that hard-sphere glasses exhibit the frozen in structure of the equilibrium liquid. Furthermore, this paper indicates that certain nonequilibrium glassy structures can be distinguished from the equilibrium liquid based on structural information alone.

A detailed analysis of jammed structures, produced by the protocol of Lubachevsky and Stillinger, indicates that there is no unambiguous division between amorphous and polycrystalline glasses. In fact, the degree of ordering in those systems (spanning from “liquidlike” to “crystal-like”) can be statistically controlled by the compression rate. That is to say, slightly denser packings can be created at the expense of arbitrarily small increases in order. Therefore, as we have demonstrated elsewhere in more detail [20], the traditional notion of the random close-packed state should be reassessed.

Finally, we have demonstrated that there is a distinct ordering phase diagram that exists for the purely repulsive hard-sphere system, whose qualitative form is reproduced by all of the order parameters investigated in this paper. Predicting how the form of this diagram depends on the details of the interactions in a given system remains a fundamental challenge to understanding ordering in condensed-phase systems.

## ACKNOWLEDGMENTS

We thank F. H. Stillinger, T. Spencer, and M. Utz for many valuable discussions and suggestions. P.G.D. gratefully acknowledges support of the U.S. Department of Energy, Division of Chemical Sciences, Office of Basic Energy Sciences (Grant No. DE-FG02-87ER13714). S.T. was supported by the Engineering Research Program of the Office of Basic Energy Sciences at the U.S. Department of Energy (Grant DE-FG02-92ER14275). T.M.T. acknowledges the support of The National Science Foundation.

- 
- [1] C. Kittel, *Introduction to Solid State Physics*, 7th ed. (Wiley, New York, 1996).  
 [2] Y. Hama, K. Suzuki, K. Shingu, M. Fujimori, S. Kobayashi, N. Usuda, and J. Amano, *Thyroid* **9**, 927 (1999).  
 [3] L. Brinon, S. Geiger, V. Alard, J. Doucet, J.-F. Tranchant, and G. Couarraze, *J. Controlled Release* **60**, 67 (1999).

- [4] R. Zallen, *The Physics of Amorphous Solids* (Wiley, New York, 1983).  
 [5] N.E. Cusack, *The Physics of Structurally Disordered Matter: An Introduction* (Adam Hilger, Bristol, 1987).  
 [6] P. Hertz, *Math. Ann.* **67**, 387 (1909).  
 [7] Lord Rayleigh, *Nature* (London) **45**, 80 (1891).

- [8] L. Tonks, Phys. Rev. **50**, 955 (1936).
- [9] Z.W. Salsburg, R.W. Zwanzig, and J.G. Kirkwood, J. Chem. Phys. **21**, 1098 (1953).
- [10] A. Robledo and J.S. Rowlinson, Mol. Phys. **58**, 711 (1986).
- [11] R.J. Speedy, J. Chem. Soc., Faraday Trans. 2 **76**, 693 (1980).
- [12] S. Torquato, B. Lu, and J. Rubinstein, Phys. Rev. A **41**, 2059 (1990).
- [13] M.D. Rintoul, S. Torquato, and G. Tarjus, Phys. Rev. E **53**, 450 (1996).
- [14] P. Viot, P.R. Van Tassel, and J. Talbot, Phys. Rev. E **57**, 1661 (1998).
- [15] T.M. Truskett, S. Torquato, and P.G. Debenedetti, Phys. Rev. E **58**, 7369 (1998).
- [16] Z. Elkoshi, H. Reiss, and A.D. Hammerich, J. Stat. Phys. **41**, 685 (1985).
- [17] D.S. Corti and P.G. Debenedetti, Phys. Rev. E **57**, 4211 (1998).
- [18] C.D. Barnes and D.A. Kofke, J. Chem. Phys. **110**, 11 390 (1999).
- [19] G.F. Kinney, *Engineering Properties and Applications of Plastics* (Wiley, New York, 1957).
- [20] S. Torquato, T.M. Truskett, and P.G. Debenedetti, Phys. Rev. Lett. **84**, 2064 (2000).
- [21] L. Pusztai and O. Gereben, Mater. Sci. Eng., A **179**, 433 (1994).
- [22] *Bond-Orientational Order in Condensed Matter Systems*, edited by K.J. Strandburg (Springer-Verlag, New York, 1992).
- [23] P.J. Steinhardt, D.R. Nelson, and M. Ronchetti, Phys. Rev. B **28**, 784 (1983).
- [24] We note that alternative neighbor definitions, such as the “geometric neighbors” that result from a Delaunay tessellation [see, e.g., M. Tanemura, T. Ogawa, N. Ogita, J. Comput. Phys. **51**, 191 (1983)] were tested and shown to give qualitatively similar results.
- [25] For a discussion of bond-orientational order parameters designed for liquid water see P.-L. Chau and A.J. Hardwick, Mol. Phys. **93**, 511 (1998).
- [26] B.D. Lubachevsky and F.H. Stillinger, J. Stat. Phys. **60**, 561 (1990).
- [27] B.D. Lubachevsky, F.H. Stillinger, and E.N. Pinson, J. Stat. Phys. **64**, 501 (1991).
- [28] A similar rate-dependent densification scheme [L.V. Woodcock, J. Chem. Soc., Faraday Trans. 2 **72**, 1667 (1976)] was introduced in 1976 to investigate the metastable hard-sphere fluid.
- [29] R.J. Speedy, Mol. Phys. **83**, 591 (1994).
- [30] C.A. Angell, J.H.R. Clarke, and L.V. Woodcock, Adv. Chem. Phys. **48**, 397 (1981).
- [31] A.L. Greer, Science **267**, 1947 (1995).
- [32] C.J. Lin and F. Spaepen, Acta Metall. **34**, 1367 (1986).
- [33] Anonymous, Nature (London) **239**, 488 (1972).
- [34] The behavior of  $Q_6$  in the hard-sphere system was studied previously by M.D. Rintoul and S. Torquato, J. Chem. Phys. **105**, 9258 (1996) in the context of crystallization from the metastable fluid. The relationship between  $Q_6$  and  $\phi$  has been revisited in more detail recently by P. Richard, L. Oger, J.-P. Troadec, and A. Gervois, Phys. Rev. E **60**, 4551 (1999) for the hard-sphere fluid (both stable and metastable), the equilibrium crystal, and the fluid-solid coexistence region.
- [35] For lack of a detailed molecular picture, the morphology of a glassy material is commonly described as resembling the “frozen in” structure of a liquid. Simple (and pedagogically useful) descriptions of this nature typically appear in introductory materials science textbooks, review articles, and research monographs [see, e.g., W.D. Callister, *Materials Science and Engineering*, 3rd ed. (Wiley, New York, 1994) p. 388; J. M. Ziman, *Models of Disorder* (Cambridge University Press, Cambridge, 1979), p. 101; C.A. Angell, Science **267**, 1924 (1995)].
- [36] T.M. Truskett, S. Torquato, S. Sastry, P.G. Debenedetti, and F.H. Stillinger, Phys. Rev. E **58**, 3083 (1998).
- [37] A.R. Kansal, T.M. Truskett, and S. Torquato (unpublished).
- [38] R.E. Nettleton and M.S. Green, J. Chem. Phys. **29**, 1365 (1958).
- [39] H. S. Green, *The Molecular Theory of Fluids* (North-Holland, Amsterdam, 1952), pp. 70–73.
- [40] A. Baranyai and D.J. Evans, Phys. Rev. A **40**, 3817 (1989).
- [41] B.B. Laird and A.D.J. Haymet, Phys. Rev. A **45**, 5680 (1992).
- [42] D.J. Evans, J. Stat. Phys. **57**, 745 (1989).
- [43] J. Yvon, *Correlations and Entropy in Classical Statistical Mechanics* (Pergamon, Oxford, 1969), pp. 71–77.
- [44] F.H. Stillinger and Z.W. Salsburg, J. Stat. Phys. **1**, 179 (1969).